An Analysis for Measurement of Thermal Diffusivity Components of Anisotropic Platelike Samples by AC Calorimetric Method

2000 Jpn. J. Appl. Phys. 39 L690

(http://iopscience.iop.org/1347-4065/39/7A/L690)

Jpn. J. Appl. Phys. Vol. 39 (2000) pp. L 690–L 693
Part 2, No. 7A, 1 July 2000

An Analysis for Measurement of Thermal Diffusivity Components of Anisotropic Platelike Samples by AC Calorimetric Method

Long-Jye SHEU and Jenn-Der LIN
Department of Mechanical Engineering, National Chiao Tung University, 1001 Ta Hsueh Rd., Hsinchu, Taiwan, R.O.C.

(Received January 17, 2000; accepted for publication May 9, 2000)

This work examines the effects of anisotropy and transparency on measurements of thermal diffusivity components with an ac calorimetric method associated with laser heating. Analytical results indicate that the region where the two-dimensional effect occurs increases with the decrease of the ratio of cross-plane to in-plane thermal diffusivity. The region also increases with the optical thickness of the sample. The linear relations, as indicated by a decay constant from which the cross-plane thermal diffusivity is deduced, are not obtained for media of both optically moderate and thin thickness, while at sufficiently large optical thickness, anisotropy and two-dimensional effects are found insignificant.

KEYWORDS: thermal diffusivity, ac calorimetric, two-dimensional, anisotropy, semi-transparent

1. Introduction

Hatta *et al.*,[1,2] Gu and Hatta,[3] Kato *et al.*[4] and Gu *et al.*[5] developed an ac calorimetric method for measuring the in-plane thermal diffusivity of a thin film. That research assumed that the ac temperature wave propagates one-dimensionally along the surface, thus allowing one to determine the thermal diffusivity by analyzing the decay curve of the ac temperature waves. The decay constant of the phase or the logarithm of the amplitude of ac temperature wave is given by $k = \sqrt{\pi f / D_x}$, where f is the frequency of the ac light and D_x is the thermal diffusivity of the material. With larger sample thickness, assuming a one-dimensional (1D) temperature distribution becomes invalid. The two-dimensional (2D) effect on the ac temperature must then be included and has been analyzed by Yamane *et al.*,[6] Hatta *et al.*[7] and Takahashi *et al.*[8] The ac calorimetric methods for measuring the cross-plane thermal diffusivity of a film have also been proposed by Yang *et al.*[9] and Kato *et al.*[10] using a one-dimensional model.

The above investigations considered the isotropic media. For anisotropic materials, the thermal diffusivity components will influence the 2D ac temperature response. Hatta[7] briefly addressed the effect of anisotropy. To further investigate the effect of anisotropy and 2D ac temperature response, this work considers a platelike sample of thickness d, for which a part of the sample surface is irradiated by uniformly distributed radiation heat while the remaining surface is shadowed by a mask. The anisotropy of the sample is considered to be orthorhombic[11] with two thermal diffusivity components, parallel and perpendicular to the sample surface. The effect of material transparency on the temperature response, as may occur with dielectric thin films during laser heating, is also included.

2. Theory

Figure 1 presents the physical model and coordinate systems, and the governing equations for temperature response are given as

$$\kappa_x \frac{\partial^2 T}{\partial x^2} + \kappa_y \frac{\partial^2 T}{\partial y^2} + q(x, y, t) = \rho c \frac{\partial T}{\partial t}, \quad (1)$$

where κ_x and κ_y are, respectively, the in-plane and cross-plane thermal conductivity components. ρ is the density and c the specific heat. The heat source term $q(x, y, t)$ can be described as

$$q(x, y, t) = Q\alpha(1 - R)\left\{ e^{-\alpha y} + \sum_{n=1}^{\infty}[R^{2n-1}e^{-\alpha(2nd-y)} + R^{2n}e^{-\alpha(2nd+y)}]\right\}[H(x + a) - H(x)]e^{i2\pi f t}, \quad (2)$$

with the multiple reflections at boundaries included. α is the absorption coefficient and R denotes the boundary reflectivity. H represents the heaviside function. Q is the heat flux per unit area of the incident beam. i is equal to $\sqrt{-1}$. f denotes the frequency of the incident beam and a represents the spatial width of the incident beam.

The initial and boundary conditions for surfaces with convection heat loss are

$$T(x, y, t) = 0 \quad \text{at} \quad t = 0, \quad (3)$$

$$T(-\infty, y, t) = T(\infty, y, t) = 0, \quad (4)$$

$$\frac{\partial T(x, 0, t)}{\partial y} - \frac{h}{\kappa_y} T(x, 0, t) = 0, \quad (5)$$

$$\frac{\partial T(x, d, t)}{\partial y} + \frac{h}{\kappa_y} T(x, d, t) = 0, \quad (6)$$

where h is the convective heat transfer coefficient. By using the Fourier transform technique and introducing the following

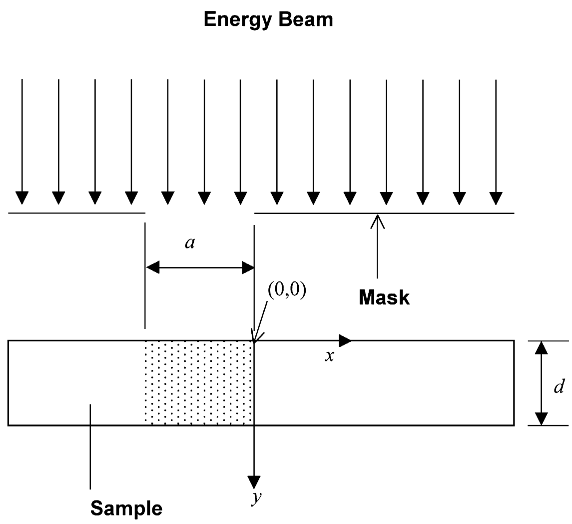

Fig. 1. Physical model and coordinate systems.

nondimensional parameters,

$$x' = \frac{x}{d/\pi}, \quad y' = \frac{y}{d/\pi}, \quad f' = \frac{f}{\pi^2 D_x/d^2},$$

$$\kappa = \frac{D_y}{D_x}, \quad \tau = \alpha d, \quad B = \frac{hd}{\kappa_x \pi}, \tag{7}$$

the ac temperature is then derived as

$$\frac{T_{ac}(x', y', f')}{Qd/2\pi^3\kappa_y} = \int_{-\infty}^{\infty} \frac{\tau(1-R)(e^{-iwa'}-1)}{iw[\tau^2/\pi^2 - (w^2 + 2\pi f' i)/\kappa]} \left[\frac{(q+B/\kappa)e^{qy'}FF - (q-B/\kappa)e^{-q(\pi-y')}EE}{(q+B/\kappa)^2 e^{q\pi} - (q-B/\kappa)^2 e^{-q\pi}} \right.$$
$$\left. \times \frac{(q-B/\kappa)e^{-qy'}FF - (q+B/\kappa)e^{q(\pi-y')}EE}{(q+B/\kappa)^2 e^{q\pi} - (q-B/\kappa)^2 e^{-q\pi}} + P(y') \right] e^{-iwx'} dw, \tag{8}$$

where the D's are the thermal diffusivity components. τ denotes the optical depth of the sample, and B represents the Biot number.

$$q = \sqrt{(w^2 + 2\pi f i)/\kappa}, \tag{9}$$

and

$$P(y') = e^{-\tau y'/\pi} + \sum_{n=1}^{\infty} [R^{2n} e^{-\tau(2n+y'/\pi)} + R^{2n-1} e^{-\tau(2n-y'/\pi)}] \tag{10}$$

with

$$EE = \left(\frac{\tau}{\pi} + \frac{B}{\kappa}\right)\left[1 + \sum_{n=1}^{\infty} R^{2n} e^{-2n\tau}\right] + \left(\frac{B}{\kappa} - \frac{\tau}{\pi}\right) \sum_{n=1}^{\infty} R^{2n-1} e^{-2n\tau} \tag{11}$$

and

$$FF = \left(\frac{\tau}{\pi} - \frac{B}{\kappa}\right)\left[e^{-\tau} + \sum_{n=1}^{\infty} R^{2n} e^{-(2n-1)\tau}\right] - \left(\frac{B}{\kappa} + \frac{\tau}{\pi}\right) \sum_{n=1}^{\infty} R^{2n-1} e^{-(2n-1)\tau}. \tag{12}$$

The solution $T_{ac}(x', y', f')$ of eq. (8) is a complex value. The amplitude $|T_{ac}(x, y, f)|$ and phase $\phi(x, y, f)$ of the ac temperature response are then obtained from

$$|T_{ac}(x', y', f')| = \sqrt{T_{RE}^2(x', y', f') + T_{IM}^2(x', y', f')}, \tag{13}$$

and

$$\phi(x', y', f') = \arctan[T_{IM}(x', y', f')/T_{RE}(x', y', f')]. \tag{14}$$

The subscripts RE and IM respectively denote the real and imaginary parts of T_{ac}.

When heat loss can be neglected, the apparent thermal diffusivity of either D_a^* or D_p^*, respectively derived from the decay of the amplitude and the shift of the phase, can be used to accurately derive the thermal diffusivity D_x.[5] To compare D_a^* and D_p^* derived from 2D temperature responses with the 1D results, both D_a^* and D_p^* are obtained as follows. The plots of $\ln|T_{ac}(x', y', f')|/\sqrt{f'}$ and $\phi(x', y', f')/\sqrt{f'}$ versus x' decay with a constant slope of $\sqrt{\pi}$ under 1D analysis,[1] and either plot would deduce the thermal diffusivity D_x. In 2D analysis, the plots of $\ln|T_{ac}(x', y', f')|/\sqrt{f'}$ and $\phi(x', y', f')/\sqrt{f'}$ versus x' decay with slopes of a_a and a_p and can deduce the apparent thermal diffusivities D_a^* and D_p^*, respectively. The nondimensional thermal diffusivity, D_a^*/D_x and D_p^*/D_x, along the x' direction is determined by[6]

$$D_a^*/D_x = \pi/a_a^2, \quad \text{and} \quad D_p^*/D_x = \pi/a_p^2. \tag{15}$$

The values of a_a and a_p at each point are derived from the partial dervatives of $\ln|T_{ac}(x', y', f')|/\sqrt{f'}$ and $\phi(x', y', f')/\sqrt{f'}$ with respect to x' for each point, i.e.,

$$a_a = \partial\{\ln|T_{ac}(x', y', f')|/\sqrt{f'}\}/\partial x', \tag{16}$$

$$a_p = \partial\{\phi(x', y', f')/\sqrt{f'}\}/\partial x'. \tag{17}$$

3. Results and Discussion

The trapezoid method is used to calculate the integral in eq. (8). In numerical computations, the limit, ∞, of the integration is replaced by 10, which has been found sufficiently large. With respect to the amplitude, a quantity of $\ln(Qd/2\kappa_y\pi^3)$ is substracted since only the relative values of $\ln|T_{ac}(x', y', f')|$ are necessary.

Figure 2(a) shows the effect of κ on the measured $\sqrt{(D_a^*/D_x)(D_p^*/D_x)}$ along x' at the back surface $y' = \pi$ for $f' = 0.00001$, $B = 0.0001$ and $R = 0.0$. The optical thickness of the sample is taken to be $\tau = 1000$, for which the sample can be regarded as opaque, making the absorption of heating energy a surface phenomenon. For isotropic materials ($\kappa = 1$), Figure 2(a) shows that in the region $x' > 6$, the values of $\sqrt{(D_a^*/D_x)(D_p^*/D_x)}$ are unity. This phenomenon implies that in this region the thermal system can be regarded as 1D. In the study of Yamane *et al.*,[6] 1D analysis for isotropic materials ($\kappa = 1$) is valid in the region where $x' > 100$. In another study of Yamane *et al.*,[11] a two-layer system was considered, on the basis of which the special case of a one-layer system was also discussed. However, their study[11] concludes that 1D is valid in the region where $x' > 10$. Our results for isotropic materials, $x' > 6$, are consistent with those of Hatta *et al.*[7] Figure 2(a) also reveals that when κ is less than 1, the value of x' when $\sqrt{(D_a^*/D_x)(D_p^*/D_x)}$ equals 1 is larger than 6, while when κ is larger than 1 the value of x' when $\sqrt{(D_a^*/D_x)(D_p^*/D_x)}$ is equal to 1 is smaller than 6. When $\kappa = 0.01$, the region where 1D analysis is valid delays to $x' > 80$. Physically, κ represents the ratio of heat wave propagation speeds in directions perpendicular and parallel to the sample surface. A large value of κ indicates that D_y is much larger than D_x and heat propagates slowly in the x-direction. Consequently, heat waves are rapidly conducted to the bottom of the sample and the thickness effect rapidly diminishes. It quickly approaches 1D analysis near the edge of the heated region. At smaller values of κ, the heat propagates faster in the

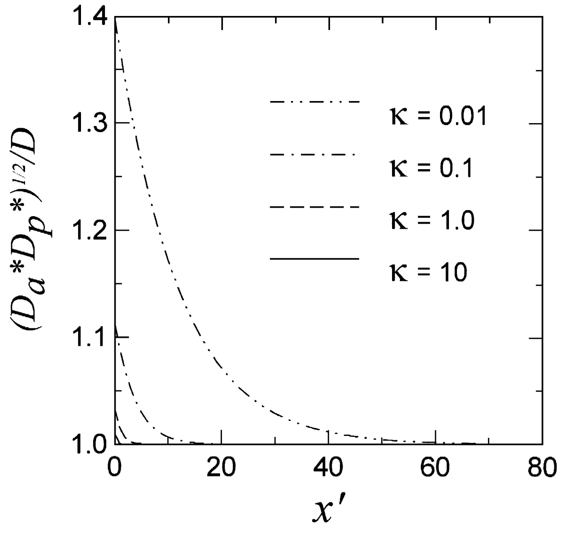

(a)

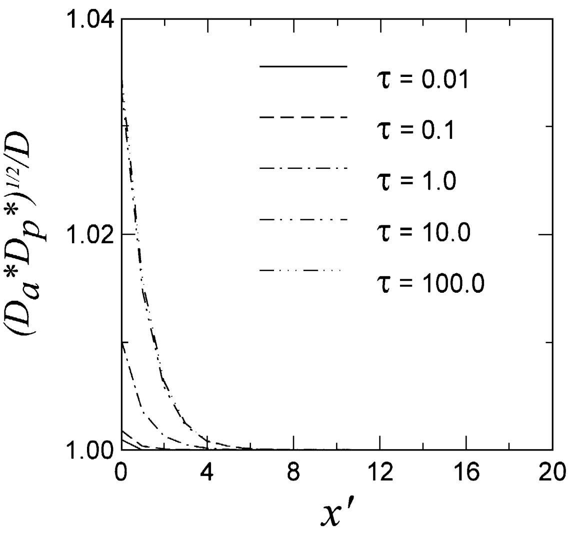

(b)

Fig. 2. Normalized thermal diffusivity estimated using eq. (15) vs x' for $f' = 0.00001$, $B = 0.0001$ and $R = 0.0$ (a) at various values of κ and $\tau = 1000$. (b) at various values of optical thickness τ and $\kappa = 1.0$.

x-direction than in the y-direction. In these cases, the effects of sample thickness become more significant and 2D distribution occurs. Experimentally, this behavior leads to a situation where the detection points should be located far from the heated region in order to obtain the true thermal diffusivity. However, the signal could be weak in such a situation, resulting in difficulty in the precise measurement of thermophysical parameters.

Figure 2(b) shows the measured $\sqrt{(D^*_{\rm a}/D_x)(D^*_{\rm p}/D_x)}$ along x' at the back surface $y' = \pi$ for $f' = 0.00001$, $B = 0.0001$, $\kappa = 1.0$ and $R = 0.0$ for semitransparent samples with various optical thicknesses, τ. Clearly, the region where the two-dimensional temperature response occurs decreases with decreasing optical thickness. The 1D propagation of the heat wave forms closer to the edge of the heated region than in the opaque samples. This phenomenon occurs because for semitransparent materials, the heating energy can penetrate into the sample medium and is directly absorbed within it, i.e., the medium is more uniformly heated across its depth within the irradiated region and thus the 1D heat propagation holds from a position close to the edge of the heated region for samples with a smaller optical thickness. Based on the analytical results for the two-dimensional temperature wave propagation, Takahashi *et al.*[8] proposed the maximum thickness required to determine thermal diffusivity for a material heated at the surface, provided that the error of the slope of the phase or amplitude distributions is within 1% at $x' = 0.5\pi/kd$. According to our results, the ac calorimetric method can be applied to semitransparent samples with thicknesses larger than those of samples calculated by Takahashi *et al.*[8] within the same error. For example, Takahashi *et al.* found the maximum thickness of a diamond sample to be 6.3 mm at $f = 1$ Hz. The absorption coefficient α of diamond is $0.11\,\mathrm{cm}^{-1}$ under a heating light with a wavelength of $0.4358\,\mu$m.[12] By considering the transparency, this study derives the maximum thickness of a diamond sample to be 13.8 mm within the same error as Takahashi *et al.* Readers may refer to ref. 12 for the absorption coefficients of various materials. For isotropic semitransparent samples, the ac calorimetric method for measuring thermal diffusivity can also avoid the photo-heating problems that occurred in the flash method[13] because the thermocouple is located outside the heating beam. The effects of boundary reflectivity, R, are also tested, indicating that this does not significantly influence the region of 2D temperature wave propagation. However, R will influence the magnitudes of the temperature waves since it affects energy absorption.

Regarding the measurement of D_y, Yang *et al.*[9] and Kato *et al.*[10] have proposed ac calorimetric methods for measuring the cross-plane thermal diffusivity. In a 1D model by Yang *et al.*,[9] the thermal diffusivity perpendicular to the sample surface is determined from the constant slope of the phase vs the square root of the frequency in the high-frequency region. The present study has noted that the ac light heating method is not suitable for determining the D_y of semitransparent samples if the thermocouples are placed under the light beam. In such conditions, photo-heating problems occur with the thermocouples. For media with sufficiently large optical thicknesses, this study assumes optical thickness τ as 1000, and the heating is then within a very small depth near the front surface and the above-mentioned linear relation may apply for parameter estimation. However, the slopes of these linear relationships depend on the value of κ. Figure 3 shows the slopes, i.e., the partial derivatives of $\phi(-a'/2, \pi, f')$, with respect to $\sqrt{f'}$ as a function of κ. Figure 3 also displays the values of the partial derivatives of $\phi(-a'/4, \pi, f')$, $\phi(0, \pi, f')$ with respect to $\sqrt{f'}$. Notably, the constant slope of the phase vs the square root of the frequency does not vary with x' as x' is under the heating beam. Thus, the value of κ can be determined from Fig. 3. With derived κ, D_y can readily be obtained by mutiplying D_x with κ. The relations between the slope and κ, as shown in Fig. 3, can be mathematically described as

$$a_{\rm sl} = 5.568/\sqrt{\kappa} = \sqrt{\pi^3/\kappa}, \tag{18}$$

where $a_{\rm sl}$ is the constant slope of the phase vs the square root of the frequency. The result of $a_{\rm sl}$ for isotropic material ($\kappa = 1$) in this study is consistent with $\sqrt{\pi^3}$ derived by Yang *et al.*[9] Equation (18) indicates that the anisotropic effect results in a multiplying factor of $1/\sqrt{\kappa}$ on $a_{\rm sl}$. In a real experiment,

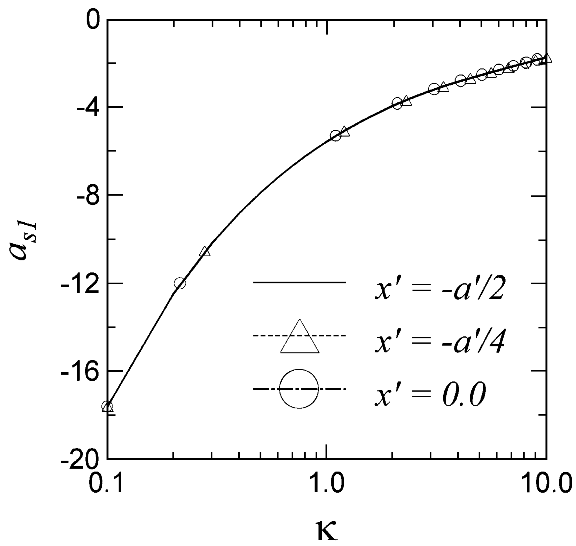

Fig. 3. Partial derivative of $\phi(x', \pi, f')$ with respect to $\sqrt{f'}$ as a function of κ.

the plot of the $\phi(-a/2, \pi, f)$ phase is derived as a function of the square root of the dimensional frequency f and the slope of the plot in a high-frequency region, for example, $a'_{\rm sl}$. Incorporating eqs. (18) and (7) produces the result of the ratio of thermal diffusivity components, $\kappa = \pi d^2/D_x a'^2_{\rm sl}$. This step then leads to the cross-plane thermal diffusivity, $D_y = \pi d^2/a'^2_{\rm sl}$. This result is consistent with the results of Yang *et al*.[9] for isotropic materials. The above analysis shows that anisotropic and 2D effects on the measurement of cross-plane thermal diffusivity are insignificant as long as the detector is located under the heating beam.

1) I. Hatta, Y. Sasuga, R. Kato and A. Maesono: Rev. Sci. Instrum. **56** (1985) 1643.
2) I. Hatta, R. Kato and A. Maesono: Jpn. J. Appl. Phys. **26** (1987) 475.
3) Y. Gu and I. Hatta: Jpn. J. Appl. Phys. **30** (1991) 1295.
4) R. Kato, A. Maesono and I. Hatta: Jpn. J. Appl. Phys. **32** (1993) 3656.
5) Y. Gu, X. Tang, Y. Xu and I. Hatta: Jpn. J. Appl. Phys. **32** (1993) L1365.
6) T. Yamane, S. I. Katayama and M. Todoki: Rev. Sci. Instrum. **66** (1995) 5305.
7) I. Hatta, K. Fujii, A. Sakibara, F. Takahashi, Y. Hamada and Y. Kaneda: Jpn. J. Appl. Phys. **38** (1999) 2988.
8) F. Takahashi, Y. Hamada and I. Hatta: Jpn. J. Appl. Phys. **38** (1999) 5278.
9) G. Yang, A. D. Migone and K. W. Johnson: Rev. Sci. Instrum. **62** (1991) 1836.
10) R. Kato, A. Maesono and I. Hatta: Jpn. J. Appl. Phys. **32** (1993) 3653.
11) T. Yamane, S. I. Katayama and M. Todoki: J. Appl. Phys. **80** (1996) 2019.
12) D. N. Nikogosyan: *Properties of Optical and Laser-Related Materials A Handbook* (John Wiley & Sons, Chichester, 1997) Chap. 3, p. 152.
13) R. S. Bretzlaff: J. Appl. Phys. **58** (1985) 2816.